A Clean-Coal Control Technology Application Study: Modelling and Control Issues for a Coal Gasifier

S. Bittanti* L. Calloni S. Canevese** A. De Marco* V. Prandoni****

** Dipartimento di Elettronica e Informazione (DEI), Politecnico di Milano, Piazza Leonardo Da Vinci 32, 20133, Milan, Italy (e-mail: sergio.bittanti@polimi.it)*
*** CESI RICERCA, Via Rubattino 54, 20134, Milan, Italy (e-mail: calloni@cesiricerca.it, canevese@cesiricerca.it, prandoni@cesiricerca.it)*

Abstract: The dynamic behaviour of a coal slurry gasifier in an Integrated Gasification Combined Cycle is modelled by means of mass, energy and momentum conservation equations as well as reaction kinetics descriptions. The main phenomena taken into consideration are (i) slurry drying and devolatilisation, (ii) char and volatile gas combustion, char gasification and water-gas shift reaction, and (iii) syngas cooling. The proposed 0-dimensional description is sufficient to capture process dynamics and it is a useful starting point for control design and verification. In particular, basic control strategies are discussed. Both model and control implementation is carried out in the Matlab-Simulink environment. Simulation results are shown to support model reliability and control effectiveness.

Keywords: Process modelling, Process automation, Process control, Process simulators, Power generation, Coal gasification.

1. INTRODUCTION

As it is well known, nowadays the scenario in electric energy production is characterised by a constant increase in demand, a decrease in fossil fuel reserves, more and more demanding restrictions on pollutant levels. Feasible solutions can be increasing efficiency and reducing pollutant emissions in thermoelectric power plants, and contributing to the development of the so called "green energy". Coal can play a major role, especially because of the important amount of its proven reserves worldwide; a main challenge for research is then to develop high-efficiency coal-based energy production systems with near zero emissions. In this paper, reference is made to a 70 MWe coal-fed Integrated Gasification Combined Cycle (IGCC) pilot plant (Fantini et al., 2007), allowing flexible production of electric energy and hydrogen. For the design, work is in progress to build up a simulator of the whole process, in order to obtain reliable predictions of its dynamic behaviour in different operating conditions and to study the operating manoeuvres. Dynamical models of the shift reactor and of the Pressure Swing Adsorption (PSA) unit have already been studied ((Bittanti et al., 2008), (Canevese et al., 2007)). Here, we focus on the gasifier, working out a first-principle model useful for control design.

In Section 2 of this paper, the gasification process is analysed, and its main phases are represented by a dynamical model, based on a thermo-fluid-dynamical and a kinetic-chemical description; such model has been developed in full detail starting from the basic conservation equations and the constitutive equations (including the kinetic equation of char gasification); here, of course, we will present only a partial outline of this model. Section 3 deals with control problems. Section 4 reports some simulation results highlighting control effectiveness. Finally, Section 5 reports some conclusions and hints to future work.

2. PROCESS ANALYSIS

The gasifier under study is an entrained-flow gasifier working at about 65 bar and 1650-1700 K. It is formed essentially by two coaxial cylinders: in the inner one, the gasification process occurs, while the outer one is employed for a first syngas cooling. As illustrated in Fig. 1, the reactor is fed with slurry (pulverized coal mixed with water which can be handled like a liquid fuel) and highly pure oxygen and it produces a gaseous mixture whose main components are CO, CO_2, H_2, N_2, H_2O, and pollutants (COS, H_2S, and dusts). We sketch the overall process of gasification and cooling as composed of the following phases (Smoot and Smith, 1985):

- *drying and devolatilisation*:

slurry can be described as coal powder where each particle is coated with a water film; when it is pumped into the inner cylinder, the high temperature that it meets makes water evaporate, thus yielding dry char, and then makes volatile gases (such as N_2, H_2S, H_2O and several kinds of hydrocarbons, among which CH_4) leave char;

- *oxidation and gasification*:

oxygen burns both the volatile gases and the char, according to the reactions

$$CH_4 + 2O_2 \rightarrow CO_2 + 2H_2O \quad (volatile\ combustion), \quad (1)$$

$$C + \left(1/\phi\right)O_2 \rightarrow 2\left(1 - 1/\phi\right)CO + \left(2/\phi - 1\right)CO_2, \quad 1 \leq \phi \leq 2 \quad (char\ combustion) \quad (2)$$

(the mechanism factor ϕ indicating whether CO or CO_2 is transported from the particle surface is calculated according to (Wen and Dutta, 1979), (van der Looij, 1988)). The related temperature increase sustains the drying and volatile emission process and the endothermic reactions

$$C + H_2O \rightarrow CO + H_2 \quad (gasification)\,, \tag{3}$$

$$C + CO_2 \rightarrow 2CO \quad (char - CO_2\ reduction)\,, \tag{4}$$

$$CO + H_2O \rightleftarrows CO_2 + H_2 \quad (water - gas\ shift)\,; \tag{5}$$

- *cooling*:

the thus obtained hot syngas (its temperature is around 1760 K) is sent to the bottom of the reactor, where contact with relatively cold liquid water causes a thermal shock which decreases the gas temperature abruptly and stops all reactions still going on; besides, unburned char residuals and char ashes solidify, fall down and are extracted as slag. After bubbling into water, the syngas is pushed by pressure difference (65 bar Vs 62 bar in the considered case) to the outer cylinder, where it is further cooled by a counter-current water spray. Spray temperature and flow rate can be used to control the outlet fluid mixture temperature and humidity. ■

Actually, the first two phases occur in the same region (gasification region). A detailed 3-D description of the phenomena taking place here is suggested, e.g., in (Chen, et al., 2000). Simpler models can be worked out by assuming that both temperature and pressure are uniform in the whole region (0-D assumption). This assumption, motivated by the intense recirculation of gases and adopted also in (Schoen, 1993) for a different type of gasifier, is adopted herein. The proposed model is able to capture the process fundamental dynamics with a low complexity degree, thus ensuring both clear physical insight and short simulation times, in view of the study of control strategies.

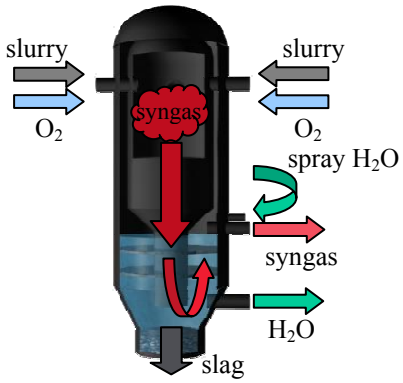

Fig. 1. The GE-Texaco gasifier: schematic view.

The following subsections report the conservation equations employed to model each phase and a reaction kinetic description for the second phase. Table 1 collects the main symbols employed.

Table 1. Nomenclature

Symbol	Description	Unit
c	Specific heat	kJ/(kg·K)
e	Relative energy	kJ/kg
f	Mass fraction	-
h	Relative enthalpy	kJ/kg
$j_k^{(r)}$	Component k stoichiometric coefficient in reaction r=1,..,5	-
p	Pressure	bar
w	Mass flow rate	kg/s
$\tilde{w}$	Molar flow rate	kmol/s
x	Molar fraction	-
A	Area	m^2
L	Length	m
M	Mass	kg
PM_k	Component k molecular weight	kg/kmol
Q	Thermal power	W
S_{ch}	Char active surface	m^2
T	Temperature	K
V	Volume	m^3
β	Mass exchange coefficient	kg/(N·s)
γ	Convective energy exchange coefficient	W/(K·m^2)
ρ	Density	kg/m^3
Ω	Equivalent perimeter	m
Subscripts		
c	Cooling region	
ch	Char	
d/u	Volume under/above the cooling liquid surface	
ev/vol	Resulting from evaporation/devolatilisation	
g/l	Gas/liquid phase	
$g\text{-}l$	Exchange between gas and liquid phases	
in/out	At the inlet/outlet of the region under study	
int/ext	Internal/external chamber	
sat	Saturation	
sh	Shift reaction	
sl	Slurry	
$surf$	Char surface	

2.1 Drying and Devolatilisation

The coal slurry injected into the gasifier forms a jet of length L_{ev} where the water evaporates heated by the hot gases. Then, after water evaporation, the volatile release takes place, due to further heating of the mass of dried coal.

The mass conservation equations for the liquid water and the dry char are respectively

$$\rho_{H_2O}\bar{A}_{H_2O}\dot{L}_{ev} = w_{sl}f_{H_2O,in} - w_{ev}\,, \tag{6}$$

$$\dot{M}_{dry} \equiv \frac{d(\rho_{dry}\bar{A}_{dry}L_{ev})}{dt} = w_{sl}(1 - f_{H_2O,in}) + \\ - M_{dry}u_j/L_{ev} + \rho_{dry}\bar{A}_{dry}\dot{L}_{ev}, \tag{7}$$

where $\bar{A}_{H_2O}$ is the evaporation average equivalent area for water and $\bar{A}_{dry}$ is the equivalent area for char,

$$w_{ev} = \beta_{g-l} L_{ev} \Omega_{ev} (p_{sat}(T_{ev}) - p_{H_2O,g}), \quad (8)$$

$L_{ev}\Omega_{ev}$ is the average evaporation surface and u_j is the particle average velocity in the drying region.

As to energy conservation, a unique average temperature T_{ev} can be adopted for the overall particle (water and char), so

$$\begin{aligned}(\rho_{H_2O}\bar{A}_{H_2O}c_{H_2O} + \rho_{dry}\bar{A}_{dry}c_{dry})[(T_{ev} - T_{sl})\dot{L}_{ev} + \\ + L_{ev}\dot{T}_{ev}] = Q_{ev} - w_{ev} \cdot (h_{g,sat}(T_{ev}) - h_{H_2O}(T_{sl})),\end{aligned} \quad (9)$$

$$Q_{ev} = \gamma_{g-l} L_{ev} \Omega_{ev} \cdot (T_g - T_{ev}). \quad (10)$$

Volatile emission is assumed to occur almost instantaneously after drying, since its dynamics are of the order of few tens of ms ((Thambimuthu and Whaley, 1987), (Kobayashi et al., 1977)); therefore, such dynamics, together with the related heating process, are neglected here. Evaporation is very fast as well, with dynamics of the order of a second at most (Thambimuthu and Whaley, 1987), so it is neglected in the simulations reported in Section 4.

2.2 Oxidation and Gasification

The mass conservation equation for the *k*-th gaseous component in the gasification volume can be written as

$$\begin{aligned}\dot{M}_k = w_{k,in} - w_{g,out} f_{k,out} + \sum_{r=2,3,4} \tilde{w}_{ch}^{(r)} PM_k j_k^{(r)} + \\ + \tilde{w}_{sh} PM_k j_k^{(5)} + \tilde{w}_{CH_4,vol} PM_k j_k^{(1)},\end{aligned} \quad (11)$$

where the component inlet flow rate is

$$w_{k,in} = \begin{cases} w_{ev}, & \text{for } k = H_2O \\ w_{k,vol}, & \text{for } k = CO_2, H_2S \\ 0, & \text{for } k = CO, H_2 \\ w_{N_2,vol} + w_{air} f_{N_2,air}, & \text{for } k = N_2 \end{cases} \quad (12)$$

and $w_{g,out} f_{k,out}$ its outlet flow rate. O_2 can be assumed to be completely consumed, and with extremely fast dynamics, by the combustion reactions (1) and (2) (Cotone, 2003); therefore, it is not necessary to write a mass conservation equation for it. For char, which is in the solid phase, we write

$$\dot{M}_{ch} = w_{dry} - \eta_g \frac{w_{g,out} M_{ch}}{\rho_g V_g} + \sum_{r=2,3,4} \tilde{w}_{ch}^{(r)} PM_{ch} j_{ch}^{(r)}, \quad (13)$$

where η_g <<1 is a shape factor (De Marco, et al., 1991) which accounts for the reaction spatial development and which can be identified from experimental results,

$$\tilde{w}_{ch}^{(r)} = \frac{K_r M_{ch} M_r}{V_{\text{int}}}, r = 3,4, M_3 = M_{H_2O}, M_4 = M_{CO_2}, \quad (14)$$

$$\tilde{w}_{ch}^{(2)} = \phi \tilde{w}_{O_2}. \quad (15)$$

$\tilde{w}_{O_2}$ is the difference between the O_2 inlet molar flow rate and the O_2 molar flow rate consumed by reaction (1). We remark that (14) is taken from the unreacted-core-shrinking model described in (Wen and Chaung, 1979); K_r accounts both for reaction kinetics, by means of an Arrhenius-type term, and for component diffusion between the gaseous bulk and the char reacting surface. The reversible shift reaction (5) kinetics is assumed to be at equilibrium on the char surface, so that the gaseous components surface diffusion is the limiting phenomenon, except for H_2, whose diffusion coefficient can be assumed as ideally infinite.

The energy conservation equations, for the gaseous mixture in the gasification volume and for solid char, read as

$$M_g c_g \dot{T}_g = Q_{g,in} - \tilde{w}_{sh} \Delta H_{sh} + w_{vol} \Delta H_{vol} + Q_{ch-g} - Q_{ev}, \quad (16)$$

$$M_{ch} c_{ch} \dot{T}_{ch} = -Q_{ch,in} + Q^{(2)} - Q^{(3)} - Q^{(4)} - Q_{ch-g}, \quad (17)$$

where

$$\begin{aligned}Q_{g,in} = w_{ev} \cdot (h_{H_2O}(T_{ev}) - h_g(T_g)) + w_{O_2} \cdot (h_{O_2}(T_{ev}) + \\ - h_g(T_g)) + w_{ev} \cdot (h_{ev}(T_{ev}) - h_g(T_g)) + w_{dry,out,vol} \cdot \\ \cdot (e_{ch}(T_{ev}) - h_g(T_g)),\end{aligned} \quad (18)$$

$$Q_{ch-g} = \gamma_{ch-g} S_{ch} \cdot (T_{ch} - T_g), \quad (19)$$

$$\begin{aligned}Q_{ch,in} = w_{dry,out,vol}(e_{ch}(T_{ch}) - e_{ch}(T_{ev})) + w_{O_2} \cdot \\ \cdot (e_{ch}(T_{ch}) - h_{O_2}(T_{ev})) + w_{ev}(e_{ch}(T_{ch}) - h_{H_2O}(T_{ev})) + \\ + w_{vol} \cdot (e_{ch}(T_{ch}) - h_{vol}(T_{ev})),\end{aligned} \quad (20)$$

$$Q^{(r)} = \tilde{w}_{ch}^{(r)} PM_{ch} \Delta H^{(r)}, r = 2,3,4 \quad (21)$$

and $\Delta H^{(2)}$ is a function of ϕ, since CO and CO_2 have different heating values.

Finally, as to pressure, the perfect gas law yields

$$p_g = \frac{R T_g}{V_g} \sum_k \frac{M_k}{PM_k}, k = H_2O, H_2, CO, CO_2, N_2, H_2S. \quad (22)$$

2.3 Cooling

The cooling volume is composed of two regions, separated by the liquid water surface: a lower "pool" region, where gas bubbles into water, and an upper spray region, where water droplets further cool humid gas leaving the pool region. Mass and energy conservation equations will be written separately for the gas mixture and for liquid water in each region.

As to the overall gas and to its water part under the surface, first of all, one can write mass conservation as

$$\dot{M}_{gd} = w_b - w_{bout} - w_{g-l}, \quad (23)$$

$$\dot{M}_{H_2O,gd} = w_b f_{H_2O,in} - w_{bout} f_{H_2O,out} - w_{g-l}, \quad (24)$$

where w_b is the gasification outlet flow rate, w_{bout} the flow rate leaving the liquid surface and w_{g-l} the exchanged (usually condensating, anyway) water flow rate inside the gas phase.

Adopting a steady-state model for the gas phase under the free liquid surface, from (23) and (24) we can write

$$w_{bout} = w_{g,out} (1 - f_{H_2O,in}) / (1 - f_{H_2O,out}) \quad (25)$$

$$w_{g-l} = w_b (f_{H_2O,out} - f_{H_2O,in}) / (1 - f_{H_2O,out}), \quad (26)$$

and, adopting an equilibrium model,

$$f_{H_2O,out} = \frac{PM_{H_2O} p_{sat}(T_{ld})}{\overline{PM_{gd}}[p_c - p_{sat}(T_{ld})] + PM_{H_2O} p_{sat}(T_{ld})}, \quad (27)$$

where $\overline{PM_{gd}}$ is the average molecular weight of the "dry" gas, i.e. without considering its water contents.

As to energy conservation, we have

$$M_g c_g \dot{T}_{gd} = Q_{g,ex} - Q_{gl} - w_b(h(p_g, T_{in}, f_{gd}) + -h(p_c, T_{gd,out}, f_{gd,out})), \quad (28)$$

$$Q_{g,ex} = w_{g-l}(h_{g,sat}(T_{ld}) - h_g(T_{gd})), \quad (29)$$

$$Q_{gl} = \gamma_{g-l} S_{g-l}(T_{gd} - T_{ld}). \quad (30)$$

In (28), the last product term in the right-hand member describes the heat lost to decrease the inlet gas temperature; p_c is the upper cooling region pressure.

As to the liquid water mass M_{ld} under the surface, one has

$$\dot{M}_{ld} = w_{H_2O\_down} + w_{g-l} - w_{ld,out}, \quad (31)$$

where the three terms on the right-hand member are due to water falling down from the cooling upper region into the pool because of gravity, to the condensating water and to the outlet water respectively. In particular,

$$w_{H_2O\_down} = M_{w\_spr} / \tau_{down}, \quad (32)$$

where the average delay factor τ_{down} (Lydersen, 1983) models the residence time (typically of the order of a few seconds) of spray water (whose mass is M_{w_spr}) in the spray region. $w_{ld,out}$ is a control variable which can be employed for level regulation, by means of a suitable valve.

For the liquid water temperature T_{ld} under the surface, one can write

$$M_l c_l \dot{T}_{ld} = -Q_{H_2O\_down} + Q_{l,ex} + Q_{gl}, \quad (33)$$

$$Q_{H_2O\_down} = w_{H_2O\_down}(h_{H_2O}(T_{lu}) - h_{H_2O}(T_{ld})), \quad (34)$$

$$Q_{l,ex} = w_{g-l}(h_{g,sat}(T_{ld}) - h_l(T_{ld})). \quad (35)$$

For gas mass conservation above the free surface, one has

$$\dot{M}_{gu} = w_{bout} - w_{gas,mix} - w_{cnd}, \quad (36)$$

where $w_{gas,mix}$ is the overall gasifier outlet syngas flow rate, which is assumed, for simplicity, to be regulated by a critical valve, and

$$w_{cnd} = \frac{6 M_{lu} \beta_{g-l,u}}{\rho_{lu} d_{drop}} \cdot \left(\frac{M_{steam} R T_{gu}}{PM_{H_2O} V_{spr}} - p_{sat}\left(\frac{T_{lu} + T_{w\_spr}}{2} \right) \right) \quad (37)$$

is due to humid gas condensation. T_{w_spr} is the spray inlet temperature, d_{drop} the average spray drop diameter (water drops are assumed as spherical), V_{spr} the spray region volume. M_{steam} can be derived from the conservation equation

$$\dot{M}_{steam} = w_{bout} f_{H_2O,out} - w_{cnd} - w_{gas,mix} M_{steam} / M_{gu}. \quad (38)$$

For gas energy conservation above the free surface, one has

$$M_g c_g \dot{T}_{gu} = -Q_{g,sc} - Q_{exch} + w_{bout}(h(T_{gd}, p_c) - h(T_{gu}, p_c)), \quad (39)$$

$$Q_{g,sc} = w_{cnd}(H_{g,sat}(T_{lu}) - h(T_{gu})), \quad (40)$$

$$Q_{exch} = \gamma_{g-l,u} S_{g-l,u}(T_{gu} - T_{lu}). \quad (41)$$

For the liquid water mass M_{lu} and temperature T_{lu} above the surface, respectively, one can write

$$\dot{M}_{lu} = -w_{H_2O,down} + w_{cnd} + w_{spr}, \quad (42)$$

$$M_l c_l \dot{T}_{lu} = Q_{l,sc} + Q_{exch} + w_{spr}(h(T_{w\_spr}) - h(T_{lu})), \quad (43)$$

where w_{spr} is the inlet spray water flow rate and

$$Q_{l,sc} = w_{cnd}(H_{g,sat}(T_{lu}) - h_l(T_{lu})). \quad (44)$$

Again, pressure in the cooling chamber can be derived from the ideal gas law:

$$p_c = R T_{gu} M_{gu} / (V_{spr} \overline{PM_{gu}}). \quad (45)$$

2.4 Model Verification

As for the coal composition and steady-state nominal conditions, we have made reference to the data published in (Cotone, 2003). The main model parameters, especially for the correlations, have been drawn from the literature as well. In particular, the K_r's in (14) have been taken from (Wen and Chaung, 1979). This way, our model has been fully specified. For its verification, the molar fractions supplied by the model have been compared with the molar fractions in the literature. In Table 2 such comparison is carried out by referring to the situation occurring after the thermal shock at T=1077 K.

Table 2. Comparison between literature data (Cotone, 2003) and simulation results at nominal steady state

	Reference data	Simulation results	Relative Error
x_{CO}	34%	38%	12%
x_{H_2O}	14.9%	13%	13%
x_{CO_2}	16%	15.9%	1%
x_{H_2}	33%	30.6%	7%
x_{N_2}	1.8%	2%	11%

3. CONTROL ISSUES FOR THE GASIFICATION PLANT

In this work, attention is focused on problems related to fulfilling the electrical network's needs, such as supplying the requested power variations, in normal operation (load following) or in emergency conditions, taking part in primary frequency control, or even contributing to secondary frequency control. In particular, the problem of coordinate control is dealt with here: the gasifier load and the global plant operating conditions are mastered so as to satisfy power requests from the electrical network, while preserving plant integrity and correct operation, of course. A simplified plant scheme is shown in Fig. 2. It is composed of three main parts: (i) the gasification island; (ii) a lower pressure system for the syngas treatment, together with thermal energy recovery; (iii) a conventional gas turbine, with its own fuel feed system

controlled by valve v_3. A valve, v_2 (or an expansor for power recovery), connects part (i) and part (ii). The symbol θ is adopted for actuator command signals.

We now focus on the problem of supplying fast and relatively large power variations, in order to fulfil the network's requests. For this purpose, the control scheme of Fig. 3 can be considered. Fast power variations are obtained by acting on valve v_3, regulating the turbine inlet flow rate (as in conventional power plants). By means of two feed-forward actions (FFW in Fig. 3), such variation results in corresponding changes in command signals θ_1 and θ_2. Signal θ_1 controls the slurry flow rate as well as the oxygen flow rate. θ_2 determines the flow rate of the outlet syngas. The two feed-forward actions have to be designed so as to keep constant pressure p_1, at the gasifier outlet, pressure p_2, at the turbine inlet, and temperature T_g inside the gasifier. To this purpose, in Fig. 3 a decentralized control scheme is proposed, where control signals θ_1 and θ_2 are adopted for the regulation of p_1 and p_2 (dashed rectangle of Fig. 3). Alternatively, one can resort to a centralized controller, here omitted for reasons of conciseness. As for T_g, the control action is manually operated and indicated in Fig. 3 by a dash-dotted rectangle.

Note that, for the overall control system, variations of θ_3 can be seen as main (measurable) disturbances.

We now conclude with some observations about the regulation problems.

Variable θ_1 acts simultaneously on the slurry and O_2 flow rates. Here the main objective is to keep constant the ratio between the two flow rates. However, these cannot be varied simultaneously, in order to avoid excessive over- or under-elongations in the gasification temperature. More precisely, when there is a load variation, the corresponding variation of the O_2 flow rate must take place with some delay after the variation of the slurry flow rate. The reason is that the oxygen reacts extremely fast, so that the temperature variation occurs abruptly. Such delay is represented in Fig. 3 as well (lag).

Let us finally consider the 2x2 MIMO system where θ_1 and θ_2 are the input signals, and p_1 and p_2 the output signals.

Conventional power plant operating experience would suggest regulating independently p_1 by the gasifier load and p_2 by valve v_2, as shown at the top of Fig. 3. However, the variables under study are rather interacting with each other: for instance, increasing the gasifier inlet load implies an increase in pressure p_1, which makes valve v_2 flow rate increase and therefore pressure p_2 increase as well. The degree of coupling is *quantitatively* captured by the relative gain matrix RGA, whose elements are not far from 0.5. Therefore, a centralized control solution, carried out by a forward decoupling technique, has been also analysed. The open-loop SISO transfer functions employed for controllers tuning have been identified from the system step responses around the chosen steady-state nominal point (see Section 2.4). Summing up, both centralized and decentralized controllers have been designed and simulated. Simulation results are reported in the subsequent section.

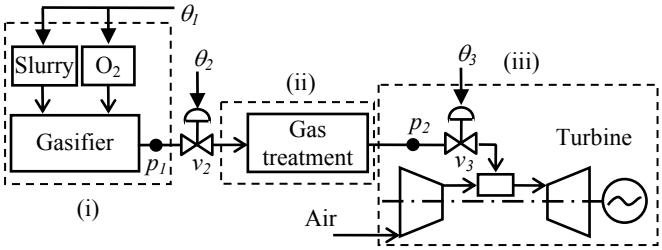

Fig. 2. The controlled simplified plant scheme.

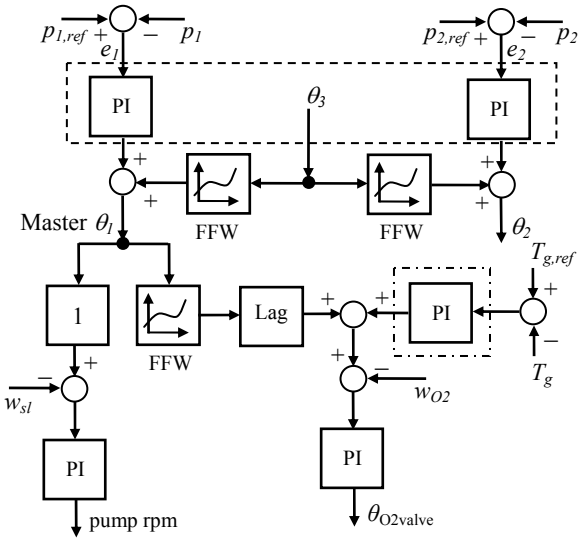

Fig. 3. A controller structure for the plant.

4. SIMULATION RESULTS

The simplified plant depicted in Fig. 2 has been simulated in the Matlab-Simulink environment, with the gasifier model, in particular, implemented by means of an S-function written in the C++ language. Simulations have been carried out both in open loop and in closed loop by considering both the centralized and the decentralized schemes. Integration has been executed in the continuous-time domain, by resorting to the standard Matlab algorithms.

Some of the results of a dynamical simulation with the centralized controller are now reported. Starting from the steady-state nominal conditions, a positive 10% step on the turbine valve position is given, at time t = 1500 s; this simulates a variation of power request from the network, so that the turbogas control system requires more inlet fuel flow rate. The top of Fig. 4 shows the responses of pressure p_1 and temperature T_g: as expected, their steady-state values are unaffected by the disturbance, and elongations around such values are very small. In Fig. 4 - bottom the control variables slurry and oxygen flow rates are depicted: they both increase in a rather slow manner, so as to preserve the integrity of the gasifier itself and of the other devices (with their dynamic operating constraints). Finally, it turns out that also the opening of valve v_2 exhibits a smooth behaviour.

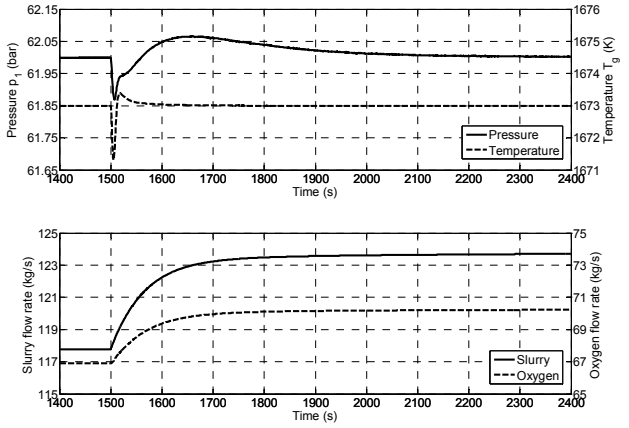

Fig. 4. Simulation results with centralized control.

5. CONCLUSIONS

A control-oriented first-principle dynamical model for a coal slurry gasifier has been proposed. Model parameters have been identified from literature data. Classical control schemes have been proposed for the 2x2 problem of controlling gasifier pressure and turbine inlet pressure by the gasifier inlet slurry and O_2 flow rates and by the gasifier outlet syngas flow rate. Simulations have shown satisfactory performance for disturbance rejection. Also the set-point tracking (not presented in this paper, for brevity) leads to good results. Future activities include model validation in transient conditions and integration of this model and models of other plant devices (see Section 1) into an overall IGCC plant simulator. Then, control strategies will be studied concerning the interaction between the gasifier and the other devices, in normal operating conditions and during startups/shutdowns; such strategies will be implemented both by standard techniques, based on SISO PID controllers, and by more involved MIMO techniques.

ACKNOWLEDGEMENTS

We are grateful to P. D'Adamo and P. De Francesco, formerly students at Politecnico di Milano, for their collaboration in the phase of parameter tuning.

This work has been financed by the Research Fund for the Italian Electrical system under the Contract Agreement between CESI RICERCA and the Ministry of Economic Development - General Directorate for Energy and Mining Resources stipulated on June 21, 2007 in compliance with the Decree n. 73 of June 18, 2007. Research has also been supported by the Italian National Research Project "New Techniques of Identification and Adaptive Control for Industrial Systems" and partially by CNR-IEIIT.

REFERENCES

Bittanti, S., Canevese, S., De Marco, A., Prandoni, V., and Serrau, D. (2008). Towards clean-coal control technologies: modelling conversion of carbon oxide into hydrogen by a shift reactor, *17th IFAC World Congress*, Seoul, South Korea.

Canevese, S., De Marco, A., Murrai, D., and Prandoni, V. (2007). Modelling and control of a PSA reactor for hydrogen purification, *ICPS'07 (1st IFAC Workshop on Convergence of Information Technologies and Control Methods with Power Plants and Power Systems)*, Cluj-Napoca, Romania.

Chen, C., Horio, M., and Kojima, T. (2000). Numerical simulation of entrained flow coal gasifiers. Part I: modeling of coal gasification in an entrained flow gasifier. *Chemical Engineering Science*, 55 (18), 3861-3874.

Cotone, P. (2003). Section D - Basic information for each alternative. In Domenichini, R., *IEA GHG Gasification power generation study, Final Report, Rev. 1*.

De Marco, A., De Michele, G., Miccio, M., Prandoni, W., and Traniello Gradassi, A. (1991). A model for the dynamic simulation of a pilot fluidized bed combustor: Predictions and first validation, *Proceedings of the 11th International Conference on Fluidized Bed Combustion*, vol. 1, 433–438. ASME, New York, NY.

Fantini, V., Mazzocchi, L., Moia, F., Prandoni, V., and Savoldelli, P. (2007). Pre-feasibility study of a flexible hydrogen-electricity co-production IGCC coal-fed plant with CO_2 capture and sequestration, *Third International Conference on Clean Coal Technologies for our Future (CCT 2007)*, Cagliari, Italy.

Kobayashi, H., Howard, J.B., and Sarofim, A.F. (1977). Coal devolatilization at high temperatures, *15th Symposium (International) on Combustion*, 16 (1), 411-425.

Lydersen, A.L. (1983). *Mass transfer in engineering practice*. John Wiley & Sons.

Schoen, P. (1993). *Dynamic modeling and control of integrated coal gasification combined cycle units*. PhD thesis, Delft University of Technology, Delft, The Netherlands.

Smoot, L.D. and Smith, P.J. (1985). *Coal combustion and gasification.* Plenum Press, New York, NY.

Thambimuthu, K.V. and Whaley, H. (1987). The combustion of coal-liquid mixtures. In C.J. Lawn (ed.), *Principles of combustion engineering for boilers*, Chapter 4, 402-408. Academic Press, London.

van der Looij, J.M.P. (1988). *Dynamic modeling and control of coal fired fluidized bed boilers*. PhD thesis, Delft University of Technology, Delft, The Netherlands.

Wen, C.Y. and Chaung, T.Z. (1979). Entrainment coal gasification modeling. *Industrial & Engineering Chemistry Process Design and Development*, 18 (4), 684-695.

Wen, C.Y. and Dutta, S. (1979). Rate of coal pyrolysis and gasification reactions. In C. Wen, Lee (ed's), *Coal conversion technology*, 57-170. Addison-Wesley Publishing Co., Reading, MA.